Iterative Robust Stabilization Algorithm for Periodic Orbits of Hybrid Dynamical Systems: Application to Bipedal Running ⋆

Kaveh Akbari Hamed * **Jessy W. Grizzle** **

* *Department of Mechanical Engineering, San Diego State University, San Diego, CA 92182 USA (e-mail: `kakbarihamed@mail.sdsu.edu`)*
** *Department of Electrical Engineering, University of Michigan, Ann Arbor, MI 48109 USA (e-mail: `grizzle@umich.edu`)*

Abstract: This paper presents a systematic numerical algorithm to design optimal $\mathcal{H}_\infty$ continuous-time controllers to robustly stabilize periodic orbits for hybrid dynamical systems in the presence of discrete-time uncertainties. A parameterized set of closed-loop hybrid systems is assumed for which there exists a common periodic orbit. The algorithm is created based on an iterative sequence of optimization problems involving Bilinear and Linear Matrix Inequalities (BMIs and LMIs). At each iteration, the optimal $\mathcal{H}_\infty$ problem is translated into a BMI optimization problem which can be easily solved using available software packages. Some sufficient conditions for the convergence of the iterative algorithm are presented. The power of the algorithm is then demonstrated in designing robust stabilizing virtual constraints for running of a highly underactuated bipedal robot with 7 degrees of underactuation in the presence of impact model uncertainties.

Keywords: Hybrid Periodic Orbits, Robust Orbital Stability, Underactuated Bipedal Running

1. INTRODUCTION

The main objective of this paper is to present a systematic numerical algorithm to design optimal $\mathcal{H}_\infty$ continuous-time controllers for robust stabilization of periodic orbits for a class of hybrid dynamical systems arising from bipedal locomotion. The robustness is achieved against uncertainty in the discrete-time dynamics of hybrid systems. Models of bipedal robots are hybrid with ordinary differential equations (ODEs) to describe stance and flight phases and discrete transitions to describe leg toe-off and impact with the ground (Hurmuzlu and Marghitu, 1994; Grizzle et al., 2014, 2001; Westervelt et al., 2007; Chevallereau et al., 2009; Ames et al., 2007; Ames, 2014; Spong and Bullo, 2005; Spong et al., 2007; Manchester et al., 2011; Dai and Tedrake, 2013; Gregg et al., 2012; Gregg and Spong, 2008; Byl and Tedrake, 2008; Akbari Hamed and Grizzle, 2014; Chevallereau et al., 2003; Morris and Grizzle, 2009; Sreenath et al., 2013; Collins et al., 2005; Byl and Tedrake, 2009; Saglam and Byl, 2013).

While the problem of designing optimal $\mathcal{H}_\infty$ controllers for complex systems is well studied in the literature (Gahinet and Apkarian, 1994; Doyle et al., 1991), existing results are tailored for stabilization of *equilibrium points* of ODEs and *not* periodic orbits of hybrid dynamical systems. The most basic tool to investigate the stability of period orbits of hybrid systems is the Poincaré sections method (Grizzle et al., 2001; Haddad et al., 2006; Parker and Chua, 1989; Haddad and Chellaboina, 2008). One of the most serious limitations in employing the Poincaré sections approach to design $\mathcal{H}_\infty$ continuous-time controllers is the lack of closed-form expressions for the Poincaré map and its Jacobian matrices. In particular, they need to be calculated numerically and this becomes a real challenge for hybrid mechanical systems with high degrees of freedom and underactuation.

Previous work in the literature made use of different approaches to stabilize hybrid periodic orbits. One of these approaches employs multi-level hybrid controller structures. In this approach, the stability of the orbit is mainly achieved by higher-level event-based controllers (Grizzle, 2006; Westervelt et al., 2007; Akbari Hamed and Grizzle, 2014; Sreenath et al., 2013). This approach may result in a potentially large delay between the occurrence of a disturbance and the event-based control effort. Other approaches employed nonlinear optimization techniques for the simultaneous design of periodic orbits and stabilizing continuous-time controllers (Chevallereau et al., 2009; Diehl et al., 2009). These approaches minimize the spectral radius of the Jacobian of the Poincaré map or a smoothed version of that and cannot address the optimal $\mathcal{H}_\infty$ control design problems. An alternative approach has been developed based on the moving Poincaré sections analysis and transverse linearization to design time (phase) varying LQR controllers (Manchester et al., 2011; Shiriaev et al., 2010). This latter approach has not been extensively evaluated on legged robots.

The contribution of this paper is to create an iterative optimization algorithm based on Bilinear and Linear Ma-

⋆ The work of K. Akbari Hamed was partially supported by the Center for Sensorimotor Neural Engineering (CSNE) that is an NSF Engineering Research Center. The work of J. W. Grizzle was supported by NSF Grants ECCS-1343720 and ECCS-1231171.

trix Inequalities (BMIs and LMIs) to design optimal $\mathcal{H}_\infty$ continuous-time controllers for hybrid models of mechanical systems with high degrees of freedom and underactuation. The algorithm acts as a powerful tool to design a general form of robust optimal nonlinear controllers including LQR and virtual constraints. Furthermore, it can be effectively solved with available software packages. Our previous work presented a non-iterative BMI optimization framework for exponential stabilization of periodic walking gaits (Akbari Hamed et al., 2014, 2015). Furthermore, a robustness analysis over two steps during stepping down/up was presented for uneven ground walking. When extending this approach to hybrid models of bipedal running, one would need to apply the BMI optimization in an iterative manner to stabilize the running gait. Furthermore, the running models are more sensitive to impact model uncertainties. This motivates us to present an iterative robust stabilization algorithm to handle $\mathcal{H}_\infty$ robustness against impact model (i.e., discrete-time) uncertainties over an infinite horizon of steps rather than two steps. To do this, the current paper presents a new BMI framework to design optimal $\mathcal{H}_\infty$ controllers. Some sufficient conditions for the convergence of the iterative algorithm in stabilizing the hybrid periodic orbits are also presented. The gait sensitivity norm was introduced in (Hobbelen and Wisse, 2007) as a disturbance rejection measure and demonstrated on a 2 DOF bipedal robot. This paper provides additional results. In regards to feedback design, the current paper presents a systematic $\mathcal{H}_\infty$ algorithm to reduce the sensitivity to impact models. Finally, the power of the algorithm is demonstrated in designing optimal $\mathcal{H}_\infty$ nonlinear controllers for a 2D underactuated bipedal runner with 7 degrees of underactuation.

2. ROBUST STABILIZATION PROBLEM

2.1 A Family of Parameterized Closed-Loop Hybrid Models

We consider a family of parameterized closed-loop hybrid systems with one continuous-time phase as follows

$$\Sigma^{\mathrm{cl}} : \begin{cases} \dot{x} = f^{\mathrm{cl}}(x,\xi), & x^- \notin \mathcal{S} \\ x^+ = \Delta(x^-,\xi) + d, & x^- \in \mathcal{S}, \end{cases} \tag{1}$$

where $x \in \mathcal{X}$ represents the state variables and $\mathcal{X} \subset \mathbb{R}^n$ is the state manifold. The continuous-time portion of the hybrid system is given by the parameterized closed-loop ODE $\dot{x} = f^{\mathrm{cl}}(x,\xi)$, in which $\xi \in \Xi \subset \mathbb{R}^p$ is a vector of adjustable constant parameters. In addition, Ξ represents a *set of admissible parameters* and the superscript "cl" stands for the closed-loop system. Here, $f^{\mathrm{cl}} : \mathcal{X} \times \Xi \to \mathrm{T}\mathcal{X}$ is a smooth (i.e., $\mathcal{C}^\infty$) vector field, in which $\mathrm{T}\mathcal{X}$ is the tangent bundle of the state manifold $\mathcal{X}$. The discrete-time portion of the dynamics is then represented by the parameterized reset law $x^+ = \Delta(x^-,\xi)+d$, where $\Delta : \mathcal{X} \times \Xi \to \mathcal{X}$ denotes a $\mathcal{C}^\infty$ *switching map*. $d \in \mathcal{D} \subset \mathbb{R}^n$ is also an *unknown* and *additive discrete-time disturbance* to represent the uncertainty in the reset model. It is further assumed that $\mathcal{D}$ contains the origin. In our notation, x^- and x^+ denote the state variables just before and after the reset event, respectively. The solutions of the hybrid system (1) undergo an abrupt change according to the reset law on the *switching manifold* $\mathcal{S}$ given by $\mathcal{S} := \{x \in \mathcal{X} \,|\, s(x) = 0\}$, where $s : \mathcal{X} \to \mathbb{R}$ is a $\mathcal{C}^\infty$ real-valued *switching function* satisfying the condition $\frac{\partial s}{\partial x}(x) \neq 0$ for

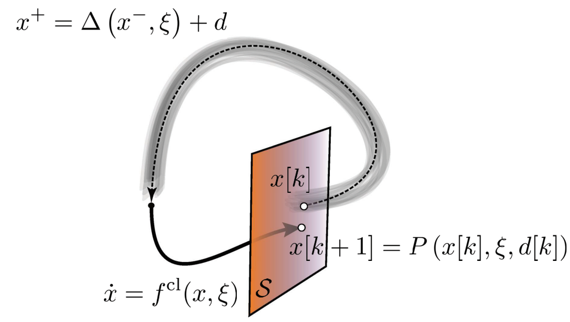

Fig. 1. Illustration of the closed-loop hybrid model (1) with one continuous-time phase. The solid and dashed curves correspond to the flows of the continuous- and discrete-time dynamics $\dot{x} = f^{\mathrm{cl}}(x,\xi)$ and $x^+ = \Delta(x^-,\xi) + d$, respectively. The uncertainty in the discrete dynamics is shown by the cloud around the dashed curve.

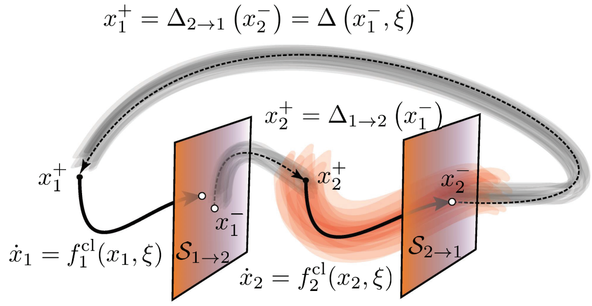

Fig. 2. Illustration of a closed-loop hybrid model with two continuous-time phases for bipedal running. Using (Grizzle et al., 2014, Proposition 4), one can present an equivalent hybrid system with one continuous-time phase as in (1), whose reset map Δ can be expressed as $\Delta := \Delta_{2\to1} \circ \mathcal{F}_2 \circ \Delta_{1\to2}$, where $\mathcal{F}_2$ denotes the flow of $\dot{x}_2 = f_2^{\mathrm{cl}}(x_2,\xi)$ (second phase) and "$\circ$" represents the composition. In this model, the uncertainty d of (1) can arise from uncertainties in $\Delta_{1\to2}$, $\Delta_{2\to1}$ and $\mathcal{F}_2$ as shown by the clouds.

all $x \in \mathcal{S}$. Figure 1 represents a geometric description for the closed-loop hybrid model (1) in the state space. Figure 2 demonstrates that the hybrid model of bipedal running with two continuous-time phases can be represented by an equivalent hybrid system with one continuous-time phase as given in (1).

The solution of the parameterized ODE $\dot{x} = f^{\mathrm{cl}}(x,\xi)$ with the initial condition $x(0) = x_0$ is denoted by $\varphi(t,x_0,\xi)$ for all $t \geq 0$ in the maximal interval of existence. The *time-to-reset* function is then defined as $T : \mathcal{X} \times \Xi \to \mathbb{R}_{>0}$ as the first time at which the ODE solution $\varphi(t,x_0,\xi)$ intersects the switching manifold $\mathcal{S}$, i.e.,

$$T(x_0,\xi) := \inf\{t > 0 \,|\, \varphi(t,x_0,\xi) \in \mathcal{S}\}. \tag{2}$$

2.2 Invariant Periodic Orbit

Throughout this paper, we shall assume that the following assumption is satisfied for the family of hybrid systems (1).

Assumption 1. It is assumed that there exists a *common* period-one orbit $\mathcal{O}$ for the family of closed-loop hybrid models in the absence of the disturbance (i.e., for $d = 0$) such that the following conditions are satisfied:

(1) Transversality: The periodic orbit $\mathcal{O}$ is *transversal* to the switching manifold $\mathcal{S}$, i.e., $\{x^*\} := \overline{\mathcal{O}} \cap \mathcal{S}$ is a singleton and $\mathrm{L}_{f^{\mathrm{cl}}} s(x^*) := \frac{\partial s}{\partial x}(x^*) f^{\mathrm{cl}}(x^*, \xi) \neq 0$ for all $\xi \in \Xi$, where $\overline{\mathcal{O}}$ represents the set closure of $\mathcal{O}$.
(2) Invariance: The periodic orbit $\mathcal{O}$ is *invariant* under the choice of closed-loop parameters ξ, i.e.,

$$\frac{\partial f^{\mathrm{cl}}}{\partial \xi}(x, \xi) = 0 \quad \forall (x, \xi) \in \mathcal{O} \times \Xi \tag{3}$$

$$\frac{\partial \Delta}{\partial \xi}(x^*, \xi) = 0 \quad \forall \xi \in \Xi. \tag{4}$$

Transversality implies that the periodic orbit $\mathcal{O}$ is *not* tangent to the switching manifold $\mathcal{S}$. In addition, invariance states that the solution of the nominal and unperturbed hybrid system (1) starting from an arbitrary point on the orbit $\mathcal{O}$ is preserved under the parameter choice. However, the parameters will be tuned to improve the robust orbital stability of the periodic orbit $\mathcal{O}$ in Section 3. If one takes the initial condition on the periodic orbit as $x_0^* := \Delta(x^*)$ and defines the invariant ODE solution by $\varphi^*(t) := \varphi(t, x_0^*, \xi)$, then the periodic orbit can be expressed as $\mathcal{O} := \{x = \varphi^*(t) \,|\, 0 \leq t < T^*\}$, where T^* is the fundamental period given by $T^* := T(x_0^*, \xi)$.

2.3 Parameterized Poincaré Map and $\mathcal{H}_\infty$ Control Problem

In order to robustly orbitally stabilize the periodic orbit $\mathcal{O}$ for the closed-loop hybrid model (1) in the presence of the unknown discrete-time disturbance $d \in \mathcal{D}$, we define a *parameterized Poincaré map* $P : \mathcal{X} \times \Xi \times \mathcal{D} \to \mathcal{X}$ by

$$P(x, \xi, d) := \varphi\left(T\left(\Delta(x, \xi) + d, \xi\right), \Delta(x, \xi) + d, \xi\right) \tag{5}$$

which describes the evolution of the closed-loop hybrid model on the Poincaré section $\mathcal{S}$ according to the following discrete-time dynamical system (see Fig. 1)

$$x[k+1] = P\left(x[k], \xi, d[k]\right), \quad k = 0, 1, 2, \cdots. \tag{6}$$

Here $\{d[k]\}_{k=0}^{\infty}$, with $d[k] \in \mathcal{D}$ for $k = 0, 1, 2, \cdots$, represents a sequence of unknown disturbances in the reset model. In addition, from the invariance condition in Assumption 1, one can conclude that x^* is an *invariant fixed point* for the Poincaré map (5) in the absence of d, that is,

$$P(x^*, \xi, 0) = x^*, \quad \forall \xi \in \Xi.$$

By defining a set of *controlled outputs* $c(x) \in \mathcal{C} \subset \mathbb{R}^r$, the discrete-time dynamical system on the Poincaré section becomes

$$\mathcal{P} : \begin{cases} x[k+1] = P\left(x[k], \xi, d[k]\right) \\ c[k] = c\left(x[k]\right) \end{cases} \tag{7}$$

for which $d[k]$ acts as an *exogenous input*. The objective is then to tune the parameter vector ξ such that (1) the fixed point x^* becomes exponentially stable for the discrete-time system (7) for $d = 0$, and (2) the effect of the disturbance d on the output c is minimized. To make this notion more precise, we linearize the dynamics (7) around $(x, d) = (x^*, 0)$ and denote the linearized system by $\partial\mathcal{P}$ as follows

$$\partial\mathcal{P} : \begin{cases} \delta x[k+1] = \dfrac{\partial P}{\partial x}(x^*, \xi, 0)\, \delta x[k] + \dfrac{\partial P}{\partial d}(x^*, \xi, 0)\, d[k] \\ \delta c[k] = \dfrac{\partial c}{\partial x}(x^*)\, \delta x[k], \end{cases} \tag{8}$$

where $\delta x[k] := x[k] - x^*$, $\delta c[k] := c[k] - c^*$, and $c^* := c(x^*)$. Next, we are interested in the following optimal $\mathcal{H}_\infty$ problem.

Problem 1. (Optimal $\mathcal{H}_\infty$ Control Problem). The optimal $\mathcal{H}_\infty$ control problem of parameter γ consists of finding the parameter vector $\xi \in \Xi$ such that

(1) the Jacobian matrix $\frac{\partial P}{\partial x}(x^*, \xi, 0)$ is Hurwitz, and
(2) the $\mathcal{H}_\infty$ norm of the transfer function relating the disturbance $d[k]$ to the output $\delta c[k]$ is less than γ, that is, $\|T_{dc}(z)\|_{\mathcal{H}_\infty} < \gamma$, in which

$$\|T_{dc}(z)\|_{\mathcal{H}_\infty} := \sup_{0 < \|d\|_2 < \infty} \frac{\|\delta c\|_2}{\|d\|_2} \tag{9}$$

is the $\mathcal{H}_\infty$ norm and $\|d\|_2 := \left(\sum_{k=0}^{\infty} d^\top[k]\, d[k]\right)^{\frac{1}{2}}$ and $\|\delta c\|_2 := \left(\sum_{k=0}^{\infty} \delta c^\top[k]\, \delta c[k]\right)^{\frac{1}{2}}$ are the $\mathcal{L}_2$ norms.

Section 3 will present an optimization algorithm to solve Problem 1 in an iterative manner.

3. ITERATIVE ROBUST STABILIZATION ALGORITHM

The objective of this section is to create an iterative optimization algorithm to overcome the curse of dimensionality and lack of closed-form expressions for the Poincaré map in designing optimal $\mathcal{H}_\infty$ continuous-time controllers. The proposed algorithm is developed based on BMIs and LMIs and generates a sequence of controller parameters $\{\xi^j\}$, where the superscript j represents the iteration number. The objective is then to converge to a set of parameters satisfying the requirements of the optimal $\mathcal{H}_\infty$ problem as stated in Problem 1. The steps of the algorithm include: (1) Sensitivity analysis, (2) BMI optimization, and (3) Iteration. In what follows, we shall address these steps.

3.1 Sensitivity Analysis

The objective of the sensitivity analysis is to make use of the first-order approximations of the state and disturbance Jacobian matrices $\frac{\partial P}{\partial x}(x^*, \xi, 0)$ and $\frac{\partial P}{\partial d}(x^*, \xi, 0)$ during each iteration to translate the optimal $\mathcal{H}_\infty$ control problem into an approximate $\mathcal{H}_\infty$ problem which can be effectively solved using a BMI optimization framework. In particular, during iteration j, based on Taylor series expansion of the Jacobian matrices around ξ^j, one can have

$$\begin{aligned} \frac{\partial P}{\partial x}\left(x^*, \xi^{j+1}, 0\right) &\approx \frac{\partial P}{\partial x}\left(x^*, \xi^j, 0\right) \\ &\quad + \sum_{i=1}^{p} \frac{\partial^2 P}{\partial \xi_i \partial x}\left(x^*, \xi^j, 0\right) \Delta\xi_i^j \\ \frac{\partial P}{\partial d}\left(x^*, \xi^{j+1}, 0\right) &\approx \frac{\partial P}{\partial d}\left(x^*, \xi^j, 0\right) \\ &\quad + \sum_{i=1}^{p} \frac{\partial^2 P}{\partial \xi_i \partial d}\left(x^*, \xi^j, 0\right) \Delta\xi_i^j, \end{aligned} \tag{10}$$

where $\Delta\xi^j := \xi^{j+1} - \xi^j := \left(\Delta\xi_1^j, \cdots, \Delta\xi_p^j\right)^\top \in \mathbb{R}^p$ is a sufficiently small increment in controller parameters. Here, the second-order derivatives $\frac{\partial^2 P}{\partial \xi_i \partial x}\left(x^*, \xi^j, 0\right) \in \mathbb{R}^{n \times n}$ and $\frac{\partial^2 P}{\partial \xi_i \partial d}\left(x^*, \xi^j, 0\right) \in \mathbb{R}^{n \times n}$ for $i = 1, \cdots, p$ are called *state* and *disturbance sensitivity matrices*, respectively. A systematic way to calculate the sensitivity matrices can be found in (Akbari Hamed et al., 2014, 2015), which relates the sensitivity matrices to the nonlinear model using the variational equation (Parker and Chua, 1989, Appendix D). Using (Akbari Hamed et al., 2014, Theorem 2), there exist matrices A_0^j, A_1^j, B_0^j and B_1^j such that the first-order approximations during iteration j can be written in the following compact forms

$$\frac{\partial P}{\partial x}\left(x^*,\xi^j,0\right)+\sum_{i=1}^{p}\frac{\partial^2 P}{\partial \xi_i \partial x}\left(x^*,\xi^j,0\right)\Delta\xi_i^j = A_0^j + A_1^j\left(I\otimes\Delta\xi^j\right) \tag{11}$$

$$\frac{\partial P}{\partial d}\left(x^*,\xi^j,0\right)+\sum_{i=1}^{p}\frac{\partial^2 P}{\partial \xi_i \partial d}\left(x^*,\xi^j,0\right)\Delta\xi_i^j = B_0^j + B_1^j\left(I\otimes\Delta\xi^j\right), \tag{12}$$

where "$\otimes$" denotes the Kronecker product. Next, by defining the constant matrix $C := \frac{\partial c}{\partial x}(x^*)$, we form the first-order approximation of dynamics (8) during iteration j as follows

$$\partial\hat{\mathcal{P}}^j : \begin{cases} \delta x[k+1] = \hat{A}\left(\xi^j,\Delta\xi^j\right)\,\delta x[k] + \hat{B}\left(\xi^j,\Delta\xi^j\right)\,d[k] \\ \delta c[k] = C\,\delta x[k], \end{cases} \tag{13}$$

in which $\hat{A}(\xi^j,\Delta\xi^j) := A_0^j + A_1^j(I\otimes\Delta\xi^j)$ and $\hat{B}(\xi^j,\Delta\xi^j) := B_0^j + B_1^j(I\otimes\Delta\xi^j)$ represent the first-order Jacobian approximations. We then present the following approximate $\mathcal{H}_\infty$ problem for robust stabilization of the origin for (13) to tune the optimal increment in controller parameters $\Delta\xi^j$.

Problem 2. (Approximate $\mathcal{H}_\infty$ Problem during Iteration j). The approximate $\mathcal{H}_\infty$ control problem of parameter γ for $\partial\hat{\mathcal{P}}^j$ consists of finding a sufficiently small increment of controller parameters $\Delta\xi^j$ such that

(1) the first-order approximation of the Jacobian matrix $\hat{A}(\xi^j,\Delta\xi^j)$ is Hurwitz, and
(2) the $\mathcal{H}_\infty$ norm of the transfer function relating $d[k]$ to $\delta c[k]$ in (13) is less than γ.

3.2 $\mathcal{H}_\infty$ BMI Optimization

The objective of this section is to translate the approximate $\mathcal{H}_\infty$ control problem during iteration j into a BMI condition. A BMI optimization problem is then set up to tune the optimal controller parameters $\Delta\xi^j$. We present the following theorem.

Theorem 1. (BMIs for the Approximate $\mathcal{H}_\infty$ Problem). For the discrete-time dynamical system (13), the following statements are equivalent:

(1) The matrix $\hat{A}\left(\xi^j,\Delta\xi^j\right)$ is Hurwitz and

$$\|T_{dc}(z)\|_{\mathcal{H}_\infty} = \left\| C\left(zI-\hat{A}\left(\xi^j,\Delta\xi^j\right)\right)^{-1}\hat{B}\left(\xi^j,\Delta\xi^j\right)\right\|_{\mathcal{H}_\infty} < \gamma.$$

(2) There exists $W = W^\top > 0$ such that the following BMI condition is satisfied

$$\begin{bmatrix} -W & W\hat{A}\left(\xi^j,\Delta\xi^j\right) & W\hat{B}\left(\xi^j,\Delta\xi^j\right) & 0 \\ \star & -W & 0 & C^\top \\ \star & \star & -\gamma^2 I & 0 \\ \star & \star & \star & -I \end{bmatrix} < 0. \tag{14}$$

Proof. See Appendix A.

Next we setup the following BMI optimization problem

$$\min_{W,\Delta\xi^j,\mu,\eta} \; \rho\,\mu + \eta \tag{15}$$

$$\text{s.t.} \quad \begin{bmatrix} -W & W\hat{A}\left(\xi^j,\Delta\xi^j\right) & W\hat{B}\left(\xi^j,\Delta\xi^j\right) & 0 \\ \star & -W & 0 & C^\top \\ \star & \star & -\mu I & 0 \\ \star & \star & \star & -I \end{bmatrix} < 0 \tag{16}$$

$$\begin{bmatrix} I & \Delta\xi^j \\ \star & \eta \end{bmatrix} > 0 \tag{17}$$

$$\eta < \eta_{\max} \tag{18}$$

$$W > 0,\; \mu > 0. \tag{19}$$

Using Schur's Lemma, the LMI condition (17) introduces the dynamic upper bound η on the norm of the increment of controller parameters as $\eta > \|\Delta\xi^j\|_2^2$ to have a good approximation based on Taylor series expansion in (10). In addition, $\eta_{\max}$ is a static upper bound on η. The BMI feasibility condition (16) guarantees the approximate $\mathcal{H}_\infty$ control condition with the parameter $\mu := \gamma^2$. The cost function (15) then minimizes a linear combination of the dynamic upper bound η and the $\mathcal{H}_\infty$ parameter μ. Finally, $\rho > 0$ is a weighting factor as a trade-off between decreasing μ and η.

3.3 Iteration

Let $(W^\star,\Delta\xi^{j\star},\mu^\star,\eta^\star)$ be a *local* [1] minimum for the BMI optimization problem (15)-(19). If the requirements of Problem 1 are satisfied at

$$\xi^{j+1} = \xi^j + \Delta\xi^{j\star} \tag{20}$$

the algorithm terminates otherwise it continues by coming back to the Sensitivity Analysis step around ξ^{j+1}. In case the BMI optimization is not feasible, then the search process is not successful and the algorithm terminates.

3.4 Sufficient Conditions for Stabilization of the Orbit

This section presents some sufficient conditions for the convergence of the iterative algorithm in stabilizing the periodic orbit at a finite number of steps. The sufficient conditions are expressed in terms of the second-order derivatives of the Jacobian matrix (i.e., third-order derivatives of the Poincaré map) and can be related to the notion of convexity. To simplify the analysis, we assume that the disturbance Jacobian matrix is zero.

Theorem 2. (Convergence of the Iterative Algorithm for Stabilization of the Hybrid Periodic Orbit) Consider the Poincaré map $P(x,\xi,d)\in\mathbb{R}^n$, in which $\xi\in\mathbb{R}^p$. Define the Jacobian matrix $A(\xi) := \frac{\partial P}{\partial x}(x^*,\xi,0)\in\mathbb{R}^{n\times n}$ and assume $B(\xi) := \frac{\partial P}{\partial d}(x^*,\xi,0) = 0$. Suppose further $a(\xi) := \mathrm{vec}(A(\xi))\in\mathbb{R}^{n^2}$ represents the vectorization of the matrix $A(\xi)$. Assume that the approximate $\mathcal{H}_\infty$ BMI problem during the iteration number j is feasible and let $\Delta\xi^{j\star}$ represent a local optimal solution (*not* necessarily the global solution). Then the following statements are correct.

[1] More details about local optimality will be presented in Remark 2.

(1) For $n > 1$, there exist $\varepsilon > 0$ and a smooth function $F : \mathbb{R}^{n^2} \to \mathbb{R}^{n+1}$ by

$$F(a) := \left(F_1(a), \cdots, F_{n+1}(a)\right)^\top$$

such that the algorithm stabilizes the origin for the discrete-time system $\delta x[k+1] = A(\xi)\,\delta x[k]$ at ξ^{j+1} (i.e., iteration $j+1$) if (1) $\|\Delta\xi^{j\star}\| < \varepsilon$ and (2) the following conditions are satisfied at $\xi = \xi^j$

$$\sum_{l=1}^{n^2} \frac{\partial F_v}{\partial a_l}(a(\xi))\,\frac{\partial^2 a_l}{\partial \xi^2}(\xi) < 0 \tag{21}$$

for $v = 1, \cdots, n+1$. In (21), $a_l(\xi)$ represents the l-th component of $a(\xi)$ and $\frac{\partial^2 a_l}{\partial \xi^2}(\xi)$ denotes the corresponding Hessian matrix.

(2) For $n = 1$, there exists $\varepsilon > 0$ such that the algorithm stabilizes the origin for the discrete-time system $\delta x[k+1] = a(\xi)\,\delta x[k]$ at ξ^{j+1} if (1) $\|\Delta\xi^{j\star}\| < \varepsilon$ and (2) the following condition is satisfied at $\xi = \xi^j$

$$a(\xi)\,\frac{\partial^2 a}{\partial \xi^2}(\xi) < 0. \tag{22}$$

Proof. See Appendix B.

Remark 1. For $n > 1$, Theorem 2 presents a set of $n+1$ LMI conditions in terms of Hessian matrices $\frac{\partial^2 a_l}{\partial \xi^2}(\xi)$ for $l = 1, \cdots, n^2$ to stabilize the periodic orbit. These conditions can be viewed as $n+1$ requirements on the convexity of the Jacobian matrix elements. For $n = 1$, theorem states some similar results. In particular, the algorithm converges if the function $a(\xi)$ is concave (resp. convex) at $\xi = \xi^j$ and $a(\xi^j) > 0$ (resp. $a(\xi^j) < 0$).

Remark 2. BMIs are NP-hard problems (Toker and Ozbay, 1995). Available software packages like PENBMI (Henrion et al., 2005) are general purpose solvers which guarantee the convergence to a critical point satisfying the first-order Karush-Kuhn-Tucker (KKT) conditions. We remark that the sufficient conditions for the convergence of the iterative algorithm in Theorem 2 do *not* require the global solution for the $\mathcal{H}_\infty$ BMI problem (15)-(19). Section 4 will illustrate the power of the algorithm by finding $\mathcal{H}_\infty$ stabilizing solutions for a hybrid system with 18 state variables and 80 controller parameters.

4. APPLICATION TO UNDERACTUATED BIPEDAL RUNNING

This section applies the results of the previous sections to design $\mathcal{H}_\infty$ stabilizing virtual constraints for a dynamic model of planar (2D) running of ATRIAS (Ramezani et al., 2013). Virtual constraints are a set of holonomic output functions defined in the configuration space of the mechanical system to coordinate the links of the robot within a stride (Grizzle et al., 2001; Westervelt et al., 2007, 2003; Freidovich et al., 2009; Ames, 2014; Akbari Hamed and Grizzle, 2014; Gregg and Sensinger, 2014; Gregg et al., 2014; Chevallereau et al., 2003, 2009; Sreenath et al., 2013; Maggiore and Consolini, 2013; Shiriaev et al., 2004). They are enforced asymptotically by continuous-time feedback control. Virtual constraint controllers have been validated experimentally for 2D and 3D walking and running robots as well as 2D powered prosthetic legs (Westervelt et al., 2007; Chevallereau et al., 2003; Sreenath et al., 2013; Buss et al., 2014; Martin et al., 2014; Ames et al., 2014; Gregg et al., 2014; Martin and Gregg, 2015). However, for mechanical systems with more than one degree of underactuation, the stability of periodic walking/running gaits depends on the choice of virtual constraints (Chevallereau et al., 2009). Previous work in the literature made use of "*physical intuition*" to design stabilizing virtual constraints (Chevallereau et al., 2009; Sreenath et al., 2013; Ramezani et al., 2013) and there was *not* any systematic algorithm to design them. In this paper, we make use of the proposed algorithm to systematically design $\mathcal{H}_\infty$ stabilizing virtual constraints. Mathematically, we are interested in the following problem.

Problem 3. (Optimal $\mathcal{H}_\infty$ Virtual Constraints). Let $\dot{x} = f(x) + g(x)\,u$ represent the Lagrangian dynamics for the hybrid model of bipedal running, where $u \in \mathcal{U} \subset \mathbb{R}^m$ denotes the continuous-time controller. Consider a family of parameterized holonomic output functions

$$y := h(x, \xi) \in \mathcal{Y} \subset \mathbb{R}^m \tag{23}$$

vanishing on the desired periodic orbit $\mathcal{O}$ with the relative degree vector being $(2, \cdots, 2)$. Let the parameterized I/O linearizing continuous-time feedback law take the form

$$u(x, \xi) = -\left(\mathrm{L}_g\,\mathrm{L}_f\,y\right)^{-1}\left(\mathrm{L}_f^2\,y + k_d\,\dot{y} + k_p\,y\right)$$

where $k_p, k_d > 0$ are positive PD gains. The optimal $\mathcal{H}_\infty$ virtual constraints problem of parameter γ then consists of finding *output parameters* ξ such that the conditions of Problem 1 are satisfied for the closed-loop hybrid model (1), in which $f^{\mathrm{cl}}(x, \xi) := f(x) + g(x)\,u(x, \xi)$.

For the purpose of this paper, the virtual constraints are expressed as

$$y = h(x, \xi) := H(\xi)\left(q - q_{\mathrm{d}}(\theta)\right),$$

in which q represents the generalized coordinates and $\theta(q)$ denotes the *phasing variable* to represent the biped's progression through the gait cycle during continuous phases. In particular, the phasing variable is strictly monotonic (i.e., strictly increasing or decreasing) scalar holonomic quantity to play the role of time in expressing the desired orbit. In addition, $q_{\mathrm{d}}(\theta)$ represents the desired evolution of the generalized coordinates on the periodic orbit $\mathcal{O}$ in terms of θ. Finally, $H(\xi)$ is an *output matrix* to be determined whose columns form the parameter vector ξ, i.e., $\xi = \mathrm{vec}(H)$.

During the stance and flight phases, ATRIAS has 9 and 11 DOFs, respectively with 4 actuators (Ramezani et al., 2013; Buss et al., 2014). In what follows, $\mathcal{O}$ is a desired periodic running gait at 1.9 (m/s) designed using the motion planning algorithm of (Sreenath et al., 2013). The nominal impact model, $x^+ = \Delta(x^-)$, assumes instantaneous rigid contacts with impulsive forces (Hurmuzlu and Marghitu, 1994; Sreenath et al., 2013). We further assume that there is a discrete-time uncertainty in the impact model denoted by $d \in \mathcal{D}$, as given in (1). An initial set of virtual constraints with the parameter vector $\xi^0 \in \mathbb{R}^{80}$ is assumed based on physical intuition to initiate the $\mathcal{H}_\infty$ iterative algorithm [2]. For this set of virtual constraints, the dominant eigenvalues of the 17×17 Jacobian of the

[2] In this paper, ξ includes the elements of the output matrices during the stance and flight phases. In particular, during the stance and flight phases, the output matrices are 4×9 and 4×11, respectively.

Poincaré map [3] and the corresponding spectral radius become $\{0.2329 \pm 0.5787i, -0.1999\}$ and 0.6238, respectively. Hence, the periodic orbit is stable. However, the $\mathcal{H}_\infty$ norm of the transfer function $T_{dc}(z)$, relating the impact model uncertainty to the COM velocity (the discrete-time output $c(x)$ is taken here as the robot's COM velocity on the Poincaré section) is 7.5930. To minimize $\|T_{dc}(z)\|_{\mathcal{H}_\infty}$, while preserving the stability of the periodic orbit, we employ the iterative BMI algorithm with the weighting factor $\rho = 0.1$ and $\eta_{\max} = 1$ (see (15)-(19)).

To solve the approximate $\mathcal{H}_\infty$ control problems (15)-(19) during each iteration of the algorithm, we make use of the PENBMI solver from TOMLAB (2015) integrated with MATLAB environment through the YALMIP (Lofberg, 2004). The BMI optimization procedure on a computer with dual 2.3 GHz Intel Xeon E5-2670 v3 processor takes approximately 20 minutes. The algorithm successfully converges to an optimized virtual constraints after 44 iterations at which the spectral radius and $\mathcal{H}_\infty$ norm of $T_{dc}(z)$ become 0.1424 and 1.8324, respectively (77% decrease in the spectral radius and 76% decrease in the $\mathcal{H}_\infty$ norm). To demonstrate the robustness of the optimal solution, Fig. 3 illustrates the x and y components of the deviation in ATRIAS' COM velocity for the nominal (i.e., initial) virtual constraints and the BMI optimized ones when a white Gaussian disturbance $d[k]$ is assumed in the velocity components of the impact model. Figure 4 depicts the phase portrait of the torso pitch angle for the $\mathcal{H}_\infty$ optimized closed-loop system during 100 consecutive running steps. Here, the simulation starts off of the orbit at the beginning of the stance phase with an initial error of +15 (deg/s) in the velocity components. Rapid convergence to the periodic orbit can be seen from the figure.

5. CONCLUSION

This paper introduced an optimization algorithm for the systematic design of optimal $\mathcal{H}_\infty$ continuous-time controllers for periodic orbits of hybrid dynamical systems. The algorithm was developed based on an iterative sequence of optimization problems involving BMIs and LMIs. The algorithm can address a general form of $\mathcal{H}_\infty$ parameterized and nonlinear feedback control schemes. It furthermore accounts for high degrees of underactuation and can be solved effectively with available software packages. The simulation results demonstrate the capability of the numerical algorithm in converging to an optimal $\mathcal{H}_\infty$ controller for a hybrid system of bipedal running with 18 state variables, 80 controller parameters, and discrete-time uncertainties in impact models. In future research, we will investigate the scalability of the algorithm and its capability in stabilizing larger size problems with a broader range of continuous- and discrete-time uncertainties. We will also investigate design of decentralized feedback controllers for underactuated bipedal robots based on the proposed algorithm.

ACKNOWLEDGEMENTS

The authors thank Dr. Brian Buss for his insightful suggestions.

[3] The 17-dimensional Poincaré map is defined at the end of the stance phase right before the leg take-off.

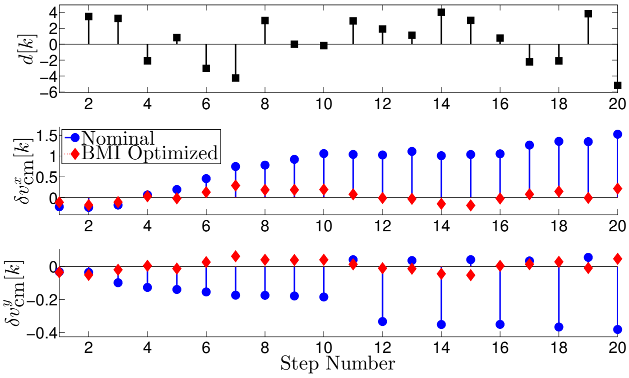

Fig. 3. Plot of a white and Gaussian discrete-time disturbance $d[k]$ (deg/s) in the velocity components of the impact model and the corresponding x and y components of the deviation in ATRIAS' COM velocity (i.e., $\delta v_{\mathrm{cm}}[k]$) (m/s) for the nominal and $\mathcal{H}_\infty$ optimized virtual constraints versus the step number k.

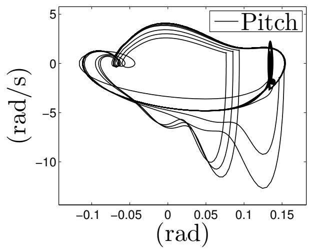

Fig. 4. Phase portrait of the pitch angle for the $\mathcal{H}_\infty$ optimized closed-loop hybrid system during 100 consecutive steps. Rapid convergence to the orbit is clear.

REFERENCES

Akbari Hamed, K., Buss, B., and Grizzle, J. (2015). Exponentially stabilizing continuous-time controllers for periodic orbits of hybrid systems: Application to bipedal locomotion with ground height variations. *The International Journal of Robotics Research*, accepted to appear.

Akbari Hamed, K. and Grizzle, J. (2014). Event-based stabilization of periodic orbits for underactuated 3-D bipedal robots with left-right symmetry. *Robotics, IEEE Transactions on*, 30(2), 365–381.

Akbari Hamed, K., Buss, B.G., and Grizzle, J.W. (2014). Continuous-time controllers for stabilizing periodic orbits of hybrid systems: Application to an underactuated 3D bipedal robot. In *Decision and Control (CDC), 2014 IEEE 53rd Annual Conference on*, 1507–1513.

Ames, A. (2014). Human-inspired control of bipedal walking robots. *Automatic Control, IEEE Transactions on*, 59(5), 1115–1130.

Ames, A., Galloway, K., Sreenath, K., and Grizzle, J. (2014). Rapidly exponentially stabilizing control Lyapunov functions and hybrid zero dynamics. *Automatic Control, IEEE Transactions on*, 59(4), 876–891.

Ames, A., Gregg, R., and Spong, M. (2007). A geometric approach to three-dimensional hipped bipedal robotic walking. In *Decision and Control, 46th IEEE Conference on*, 5123–5130.

Buss, B.G., Ramezani, A., Akbari Hamed, K., Griffin, B.A., Galloway, K.S., and Grizzle, J.W. (2014). Preliminary walking experiments with underactuated 3D bipedal robot MARLO. In *Intelligent Robots and Systems, IEEE/RSJ International Conference on*, 2529–2536.

Byl, K. and Tedrake, R. (2008). Approximate optimal control of the compass gait on rough terrain. In *Robotics and Automation. IEEE International Conference on*, 1258–1263.

Byl, K. and Tedrake, R. (2009). Metastable walking machines. *The International Journal of Robotics Research*, 28(8), 1040–1064.

Chevallereau, C., Abba, G., Aoustin, Y., Plestan, F., Westervelt, E., Canudas-de Wit, C., and Grizzle, J. (2003). Rabbit: a testbed for advanced control theory. *Control Systems, IEEE*, 23(5), 57–79.

Chevallereau, C., Grizzle, J., and Shih, C.L. (2009). Asymptotically stable walking of a five-link underactuated 3-D bipedal robot. *Robotics, IEEE Transactions on*, 25(1), 37–50.

Collins, S., Ruina, A., Tedrake, R., and Wisse, M. (2005). Efficient bipedal robots based on passive-dynamic walkers. *Science*, 307(5712), 1082–1085.

Dai, H. and Tedrake, R. (2013). L2-gain optimization for robust bipedal walking on unknown terrain. In *Robotics and Automation, IEEE International Conference on*, 3116–3123.

Diehl, M., Mombaur, K., and Noll, D. (2009). Stability optimization of hybrid periodic systems via a smooth criterion. *Automatic Control, IEEE Transactions on*, 54(8), 1875–1880.

Doyle, J., Packard, A., and Zhou, K. (1991). Review of LFTs, LMIs, and mu;. In *Decision and Control, 1991., Proceedings of the 30th IEEE Conference on*, 1227–1232 vol.2.

Freidovich, L., Mettin, U., Shiriaev, A., and Spong, M. (2009). A passive 2-DOF walker: Hunting for gaits using virtual holonomic constraints. *Robotics, IEEE Transactions on*, 25(5), 1202–1208.

Gahinet, P. and Apkarian, P. (1994). A linear matrix inequality approach to $\mathcal{H}_\infty$ control. *International Journal of Robust & Nonlinear Control*, 4(4), 421–448.

Gregg, R., Lenzi, T., Hargrove, L., and Sensinger, J. (2014). Virtual constraint control of a powered prosthetic leg: From simulation to experiments with transfemoral amputees. *Robotics, IEEE Transactions on*, 30(6), 1455–1471.

Gregg, R. and Sensinger, J. (2014). Towards biomimetic virtual constraint control of a powered prosthetic leg. *Control Systems Technology, IEEE Transactions on*, 22(1), 246–254.

Gregg, R. and Spong, M. (2008). Reduction-based control with application to three-dimensional bipedal walking robots. In *American Control Conference*, 880–887.

Gregg, R., Tilton, A., Candido, S., Bretl, T., and Spong, M. (2012). Control and planning of 3-D dynamic walking with asymptotically stable gait primitives. *Robotics, IEEE Transactions on*, 28(6), 1415–1423.

Grizzle, J.W. (2006). Remarks on event-based stabilization of periodic orbits in systems with impulse effects. In *Second International Symposium on Communication, Control and Signal Processing*.

Grizzle, J.W., Chevallereau, C., Sinnet, R.W., and Ames, A.D. (2014). Models, feedback control, and open problems of 3D bipedal robotic walking. *Automatica*, 50(8), 1955–1988.

Grizzle, J., Abba, G., and Plestan, F. (2001). Asymptotically stable walking for biped robots: analysis via systems with impulse effects. *Automatic Control, IEEE Transactions on*, 46(1), 51–64.

Haddad, W. and Chellaboina, V. (2008). *Nonlinear Dynamical Systems and Control: A Lyapunov-Based Approach*. Princeton University Press.

Haddad, W., Chellaboina, V., and Nersesov, S. (2006). *Impulsive and Hybrid Dynamical Systems: Stability, Dissipativity, and Control*. Princeton University Press.

Henrion, D., Lofberg, J., Kocvara, M., and Stingl, M. (2005). Solving polynomial static output feedback problems with PENBMI. In *Decision and Control, and European Control Conference. 44th IEEE Conference on*, 7581–7586.

Hobbelen, D. and Wisse, M. (2007). A disturbance rejection measure for limit cycle walkers: The gait sensitivity norm. *Robotics, IEEE Transactions on*, 23(6), 1213–1224.

Hurmuzlu, Y. and Marghitu, D.B. (1994). Rigid body collisions of planar kinematic chains with multiple contact points. *The International Journal of Robotics Research*, 13(1), 82–92.

Lofberg, J. (2004). YALMIP : a toolbox for modeling and optimization in MATLAB. In *Computer Aided Control Systems Design, 2004 IEEE International Symposium on*, 284–289.

Maggiore, M. and Consolini, L. (2013). Virtual holonomic constraints for Euler Lagrange systems. *Automatic Control, IEEE Transactions on*, 58(4), 1001–1008.

Manchester, I.R., Mettin, U., Iida, F., and Tedrake, R. (2011). Stable dynamic walking over uneven terrain. *The International Journal of Robotics Research*, 30(3), 265–279.

Martin, A.E., Post, D.C., and Schmiedeler, J.P. (2014). The effects of foot geometric properties on the gait of planar bipeds walking under HZD-based control. *The International Journal of Robotics Research*, 33(12), 1530–1543.

Martin, A. and Gregg, R. (2015). Hybrid invariance and stability of a feedback linearizing controller for powered prostheses. In *American Control Conference*. Accepted to appear.

Morris, B. and Grizzle, J. (2009). Hybrid invariant manifolds in systems with impulse effects with application to periodic locomotion in bipedal robots. *Automatic Control, IEEE Transactions on*, 54(8), 1751–1764.

Parker, T. and Chua, L. (1989). *Practical Numerical Algorithms for Chaotic Systems*. Springer.

Ramezani, A., Hurst, J., Akbai Hamed, K., and Grizzle, J. (2013). Performance analysis and feedback control of ATRIAS, a three-dimensional bipedal robot. *Journal of Dynamic Systems, Measurement, and Control December, ASME*, 136(2).

Saglam, C. and Byl, K. (2013). Switching policies for metastable walking. In *Decision and Control, IEEE 52nd Annual Conference on*, 977–983.

Shiriaev, A., Sandberg, A., and Canudas de Wit, C. (2004). Motion planning and feedback stabilization of periodic orbits for an acrobot. In *Decision and Control. 43rd IEEE Conference on*, volume 1, 290–295 Vol.1.

Shiriaev, A., Freidovich, L., and Gusev, S. (2010). Transverse linearization for controlled mechanical systems with several passive degrees of freedom. *Automatic Control, IEEE Transactions on*, 55(4), 893–906.

Spong, M. and Bullo, F. (2005). Controlled symmetries and passive walking. *Automatic Control, IEEE Transactions on*, 50(7), 1025–1031.

Spong, M., Holm, J., and Lee, D. (2007). Passivity-based control of bipedal locomotion. *Robotics Automation Magazine, IEEE*, 14(2), 30–40.

Sreenath, K., Park, H.W., Poulakakis, I., and Grizzle, J. (2013). Embedding active force control within the compliant hybrid zero dynamics to achieve stable, fast running on mabel. *The International Journal of Robotics Research*, 32(3), 324–345.

Toker, O. and Ozbay, H. (1995). On the NP-hardness of solving bilinear matrix inequalities and simultaneous stabilization with static output feedback. In *American Control Conference, Proceedings of the 1995*, volume 4, 2525–2526 vol.4.

TOMLAB (2015). `http://tomopt.com/tomlab/`.

Westervelt, E., Grizzle, J., Chevallereau, C., Choi, J., and Morris, B. (2007). *Feedback Control of Dynamic Bipedal Robot Locomotion*. Taylor & Francis/CRC.

Westervelt, E., Grizzle, J., and Koditschek, D. (2003). Hybrid zero dynamics of planar biped walkers. *Automatic Control, IEEE Transactions on*, 48(1), 42–56.

Appendix A. PROOF OF THEOREM 1

Pre and post multiplying the inequality (14) by the block diagonal matrix

$$\text{block diag}\{W^{-1}, I, I, I\}$$

and next applying Schur's Lemma on the result yield

$$\begin{bmatrix} \hat{A}^\top W \hat{A} - W & \hat{A}^\top W \hat{B} & C^\top \\ \star & \hat{B}^\top W \hat{B} - \gamma^2 I & 0 \\ \star & \star & -I \end{bmatrix} < 0.$$

The remaining of the proof is according to the discrete-time version of the Bounded Real Lemma provided in (Gahinet and Apkarian, 1994; Doyle et al., 1991) .

Appendix B. PROOF OF THEOREM 2

Part (1). Using a procedure analogous to that presented in Appendix A, it can be shown that the matrix inequality [4]

$$\begin{bmatrix} -W & WA & 0 & 0 \\ \star & -W & 0 & I \\ \star & \star & -\mu I & 0 \\ \star & \star & \star & -I \end{bmatrix} < 0$$

for $\mu > 0$ is equivalent to matrix $A \in \mathbb{R}^{n\times n}$ being Hurwitz. Using Jury stability criterion, one can present a set of $n+1$ scalar smooth conditions on the elements of the A matrix to have the roots of the characteristic polynomial $\lambda(z) := \det(zI - A) = 0$ inside the unit circle. These conditions can be expressed as $F(a) < 0$, where $a := \text{vec}(A)$ and "vec" denotes the vectorization operator. Two of these conditions correspond to $\lambda(1) > 0$ and $(-1)^n\lambda(-1) > 0$ which are smooth in terms of a. Hence, we choose

$$F_1(a) := -\det(I - A) < 0$$
$$F_2(a) := (-1)^{n+1}\det(-I - A) < 0.$$

[4] Without loss of generality we assume that the output is taken as $c(x) := x$.

For $n > 1$, the remaining $n-1$ conditions correspond to the Jury array and can be expressed as

$$|\alpha_i(a)| < |\beta_i(a)|, \quad i = 1, 2, \cdots, n-1, \tag{B.1}$$

where $\alpha_i(a)$ and $\beta_i(a)$ are smooth functions in terms of a. To form the corresponding components of F, one can rewrite condition (B.1) as

$$F_{i+2}(a) := \left(\alpha_i(a)\right)^2 - \left(\beta_i(a)\right)^2 < 0, \quad i = 1, 2, \cdots, n-1 \tag{B.2}$$

to make F smooth in terms of a. Next, let

$$\hat{a}(\xi, \Delta\xi) := a(\xi) + \frac{\partial a}{\partial \xi}(\xi)\,\Delta\xi \in \mathbb{R}^{n^2}$$

represent the first-order approximation of the vector $a(\xi + \Delta\xi)$. Since the approximate problem during iteration j is feasible, we have

$$F\left(\hat{a}\left(\xi^j, \Delta\xi^{j\star}\right)\right) < 0.$$

Introduce the error function

$$E(\Delta\xi) := F\left(a\left(\xi^j + \Delta\xi\right)\right) - F\left(\hat{a}\left(\xi^j, \Delta\xi\right)\right) \in \mathbb{R}^{n+1} \tag{B.3}$$

for which $E(0) = 0$ and $\frac{\partial E}{\partial \Delta\xi}(0) = 0$. A set of sufficient conditions to terminate the algorithm at $\xi = \xi^{j+1}$ is that the error function $E(\Delta\xi)$ reaches a local maximum at $\Delta\xi = 0$ so that $E(\Delta\xi) \le 0$ for sufficiently small $\|\Delta\xi\|$ or

$$F\left(a\left(\xi^j + \Delta\xi\right)\right) \le F\left(\hat{a}\left(\xi^j, \Delta\xi\right)\right) < 0.$$

It can be shown that for $v = 1, \cdots, n+1$

$$\frac{\partial E_v}{\partial \Delta\xi}(\Delta\xi) = \sum_{l=1}^{n^2} \frac{\partial F_v}{\partial a_l}\left(a\left(\xi^j + \Delta\xi\right)\right)\frac{\partial a_l}{\partial \xi}\left(\xi^j + \Delta\xi\right) - \sum_{l=1}^{n^2} \frac{\partial F_v}{\partial a_l}\left(\hat{a}\left(\xi^j, \Delta\xi\right)\right)\frac{\partial a_l}{\partial \xi}\left(\xi^j\right)$$

which in turn with some straightforward calculations results in

$$\frac{\partial^2 E_v}{\partial \Delta\xi^2}(0) = \sum_{l=1}^{n^2} \frac{\partial F_v}{\partial a_l}\left(a\left(\xi^j\right)\right)\frac{\partial^2 a_l}{\partial \xi^2}\left(\xi^j\right).$$

Hence, if the requirements at (21) are satisfied at $\xi = \xi^j$, then the Hessian matrices become negative definite, i.e.,

$$\frac{\partial^2 E_v}{\partial \Delta\xi^2}(0) < 0, \quad v = 1, \cdots, n+1,$$

and sufficient optimality conditions are met at $\Delta\xi = 0$. Hence, there is $\varepsilon > 0$ such that $E(\Delta\xi) \le E(0) = 0$ for all $\|\Delta\xi\| < \varepsilon$ and in particular for $\Delta\xi = \Delta\xi^{j\star}$. This completes the proof of Part (1).

Part (2). In the scalar case, the origin is exponentially stable for $\delta x[k+1] = a(\xi)\,\delta x[k]$ if and only if

$$F(a) := a^2 - 1 < 0.$$

Defining an error function like (B.3) and analysis analogous to that presented in Part (1) result in the following sufficient conditions for $\Delta\xi = 0$ being a local maximum

$$\frac{\partial^2 E}{\partial \Delta\xi^2}(0) = \frac{\partial F}{\partial a}\left(a\left(\xi^j\right)\right)\frac{\partial^2 a}{\partial \xi^2}\left(\xi^j\right) = 2a\left(\xi^j\right)\frac{\partial^2 a}{\partial \xi^2}\left(\xi^j\right) < 0.$$

This completes the proof of Part (2).